Synthesis of ternary nanofluids and optimization of their thermophysical properties using artificial neural network

Ganesh Veeraraghavan[1], Pushpavanam Subramaniam[2]* & Mathur Rajesh[1]*

[1]Department of Chemical Engineering, College of Engineering and Technology, SRM Institute of Science and Technology, Kattankulathur, Tamil Nadu-603203, India

[2]Department of Chemical Engineering, Indian Institute of Technology Madras, Chennai, Tamil Nadu-600036, India

*E-mail: spush@iitm.ac.in (PS); rajeshm@srmist.edu.in (MR)

1. Real-time images related to the work. (Fig. S1 – S5)

1a. S1 represents the collection of images of nanofluids synthesized at different concentrations:

(a) Synthesized Silver nanoparticles in water

(b) Synthesized hybrid nanofluid (0.005 volume fraction)

(c) Synthesized hybrid nanofluid (0.03 volume fraction)

S1: Realtime images of nanofluids synthesized

1b. S2- S5 represents the real-time lab images of the Characterization Instruments employed in the current work.

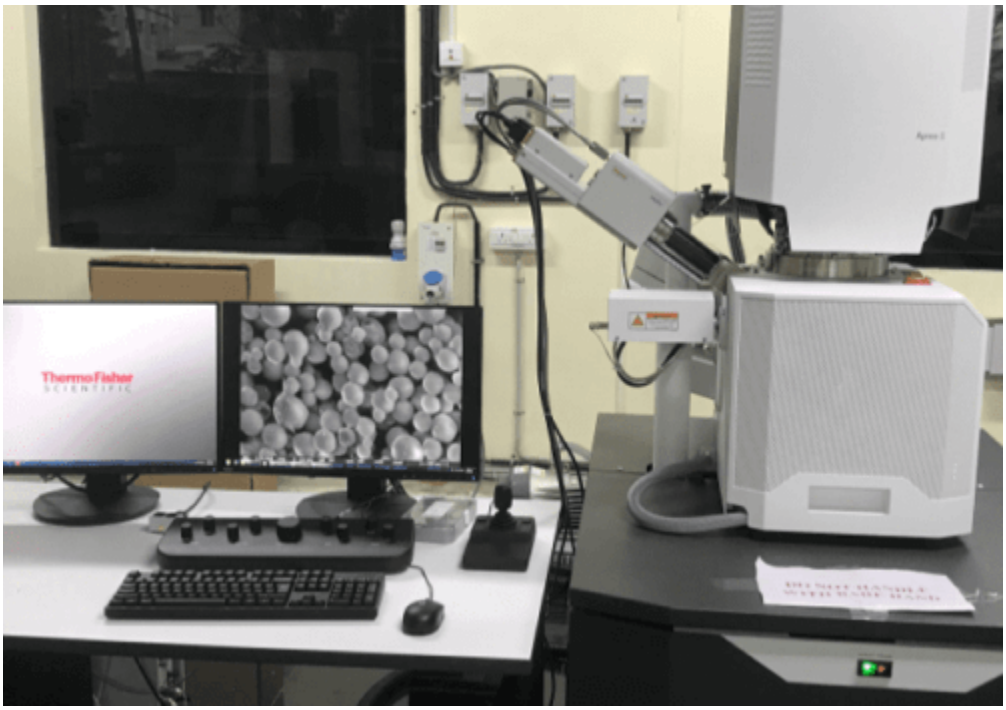

S2: HRSEM: *ThermoScientific Apreo S, ThermoFisher*

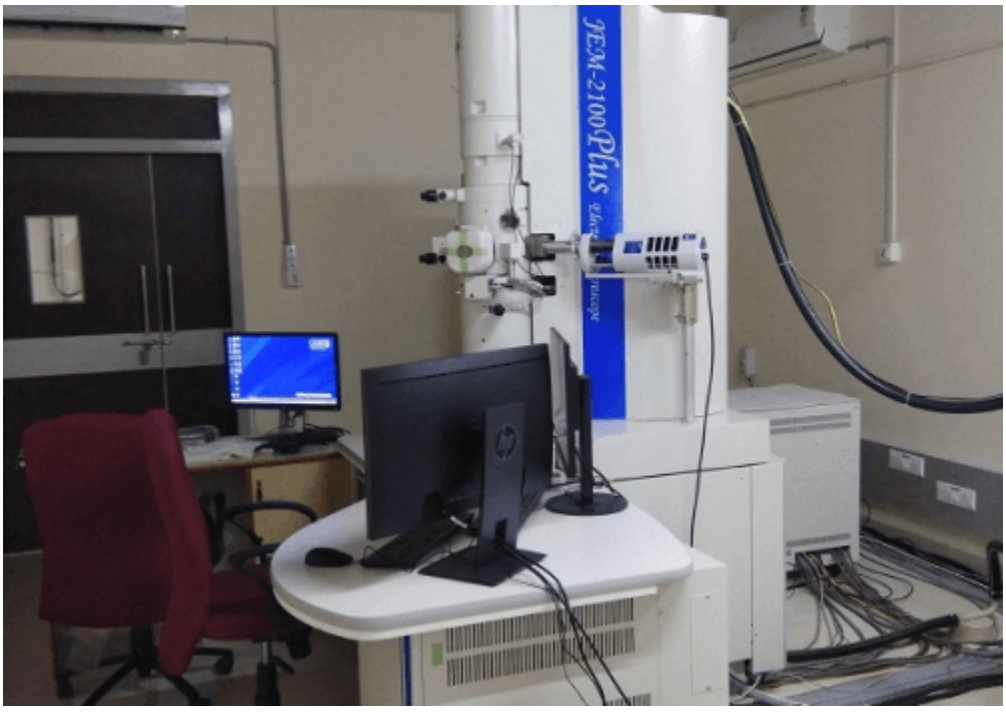

S3: HRTEM: *JEM-2100 Plus, JEOL Ltd, Japan*

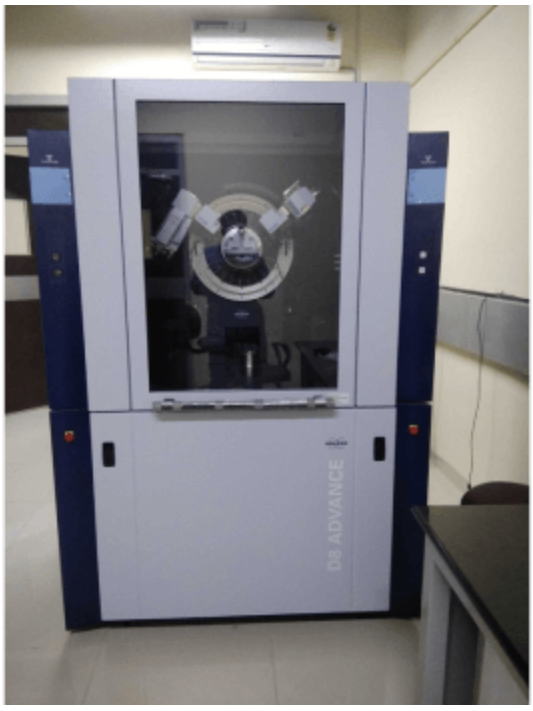

S4: XRD: ***D8 ADVANCE, Davinci, Bruker USA***

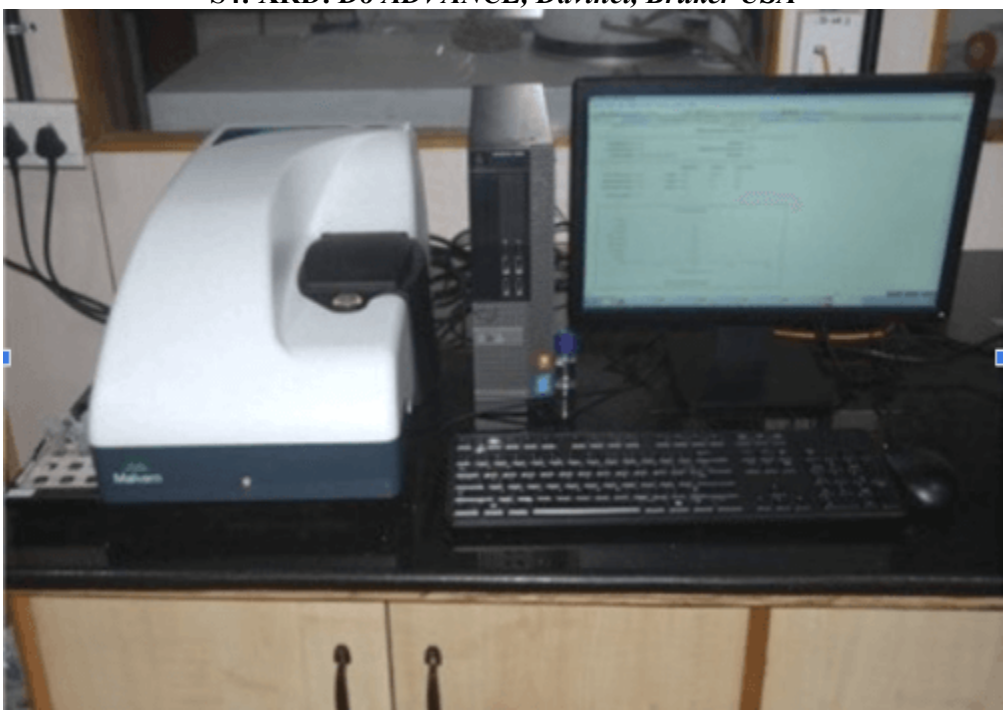

S5: Zeta Potential: ***Nano ZS-90, Malvern***

2. Work Flow (Fig S6)

The overall flow of work involved in the current study is given in S6. The authors wish to state that the overall objective of our research is the application of the synthesized nanofluids in microchannel heat transfer and evaluate their thermal performance, as part of the solution to electronics cooling.

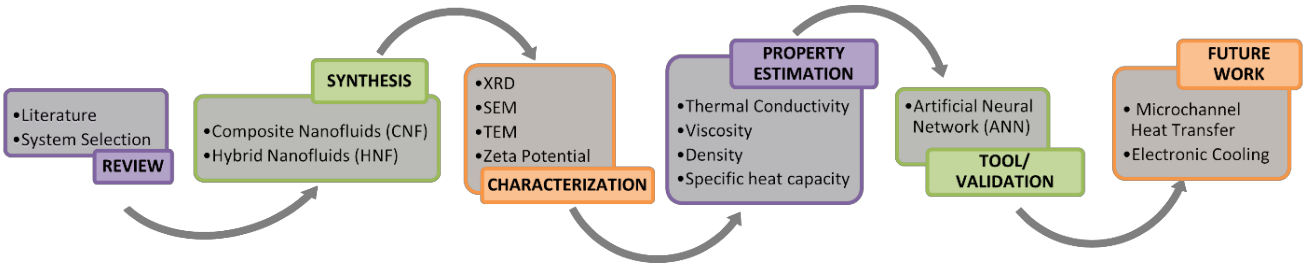

S6: Overview of the workflow

3. Literature overview of works on ternary nanofluids with details of synthesis, characterization, stability, and application

Author(s)	(Mohammed Zayan et al., 2023)	(Adun et al., 2021)	(Cakmak et al., 2020)	(Muzaidi et al., 2021)	(Ahmed et al., 2021)
Nanofluid(s)	GO-Ag-TiO_2/ DW; rGO-Ag-TiO_2/ DW	Al_2O_3-ZnO-Fe_3O_4/W; Al_2O_3-ZnO/ W	rGO-Fe_3O4-TiO2/EG	Cu-TiO2-SiO_2/W-EG	ZnO-Al_2O_3-TiO_2/ DW
Concentrations	0.0005, 0.001, 0.005, 0.01, 0.05 vol%	1 vol%	0.01, 0.05, 0.1, 0.15, 0.2, 0.25 wt%	0.04 M, 0.08 M, 0.17M	0.025, 0.05, 0.075, 0.1 wt%
SEM/TEM	Spherical Ag and TiO_2 nanoparticles embedded on GO sheets revealed.	Spherical morphology of Al_2O_3, ZnO and Fe_3O_4 nanoparticles revealed.	TiO_2 and Fe_3O_4 spherical molecules embedded on GO sheets observed.	Spherical morphology of Cu, TiO_2,SiO_2 revealed.	Spherical morphology of ZnO, Al_2O_3 and TiO_2 particles observed.
XRD	TiO_2 (anatase phase) and crystalline Ag identified.	Presence of Al_2O_3, ZnO and Fe_3O_4 nanoparticle crystals confirmed.	Peaks for GO, anatase TiO_2 and crystalline Fe_3O_4 detected	Peaks for monoclinical CuO, anatase TiO_2 and SiO_2 identified	Nil
FTIR	Following functional group vibrations were identified: C=O, C-C, C-O, C-O-H, (NH) C=O, Ag, Ti-O=Ti, Ti-O-C.	Nil	Following functional group vibrations were identified: C=O-OH, C-O-C, C=O, C=C, C-OH, O-H, Ti-O, Fe-O.	Nil	Nil
DLS	Average particle sizes 750 nm (GO-based) and 1750 nm (rGO-based)	Average particle size 90 nm for the ternary sample; 78 nm for the binary sample.	Nil	Nil	Nil
Zeta Potential	25-35mV for both	-30mV (ternary); +39mV (binary).	>52.43mV	Nil	Nil

Thermal Conductivity	10% thermal conductivity enhancement at 25^{o}C, 60% enhancement at 50^{o}C	Optimum values 0.814 (ternary) and 0.794 (binary)	Highest enhancement 13.3% observed at 60^{o}C for the 0.25 wt% sample.	Nil	Highest value of effective thermal conductivity 1.131 observed at the highest concentration (0.1 wt%).
Applications	Heat transfer fluid for thermal conductivity enhancement	Cooling fluid in PV and PV/T systems	Heat transfer and biomedical engineering	Solar thermal applications at heat absorption fluids	Energy transport
Novel features studied	Possible role of particle aggregation in thermal performance enhancement by creating a path for lower thermal resistance hypothesized. Decreased viscosity at higher temperatures associated with bond withering.	Calculation of useful energy, electrical & thermal efficiency in PV and PV/T systems. Comparison of the performance between ternary, binary and mono nanofluids.	Heat transfer enhancement of ternary hybrid compared to its constituent mono dispersions, in the experimental test rig.	It is hypothesized that the increase in temperature output with increase in solar thermal radiation is due to particle excitation, which results in greater capacity for heat absorption.	The effect of thermal diffusivity over thermal conductivity and local/average heat transfer coefficient is studied.

4. Additional Images of SEM, TEM analysis: (Fig. S7 – S15)

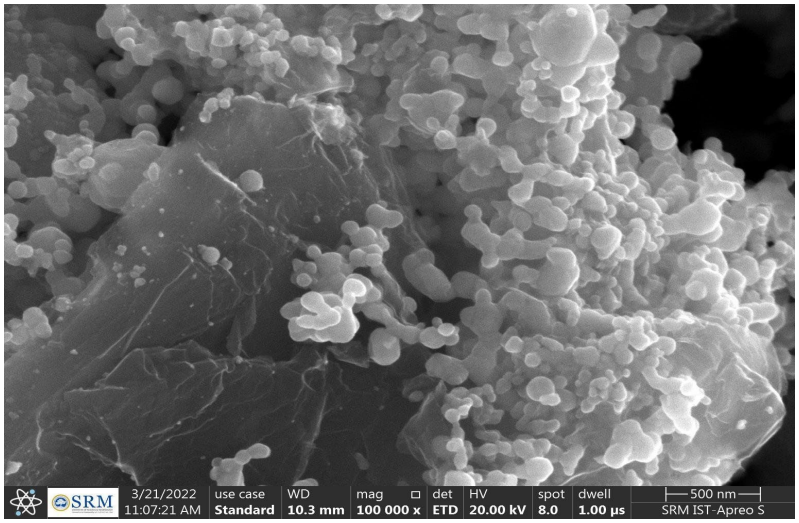

S7: SEM Micrograph at 100000x magnification

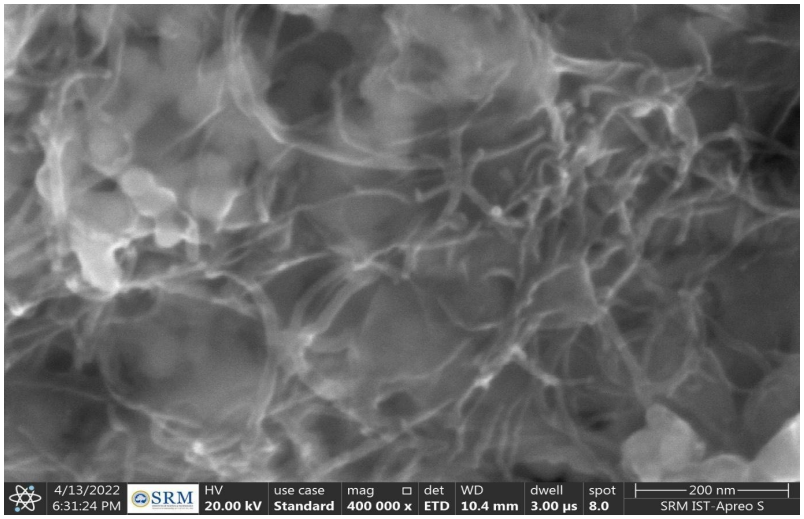

S8: SEM Micrograph at 400000x magnification

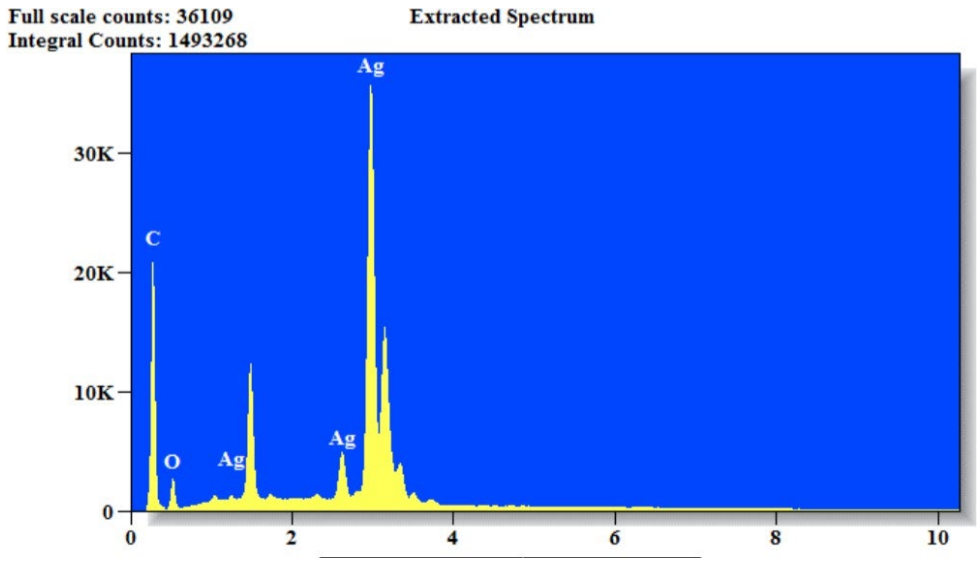

S9: EDS spectrum for the SEM

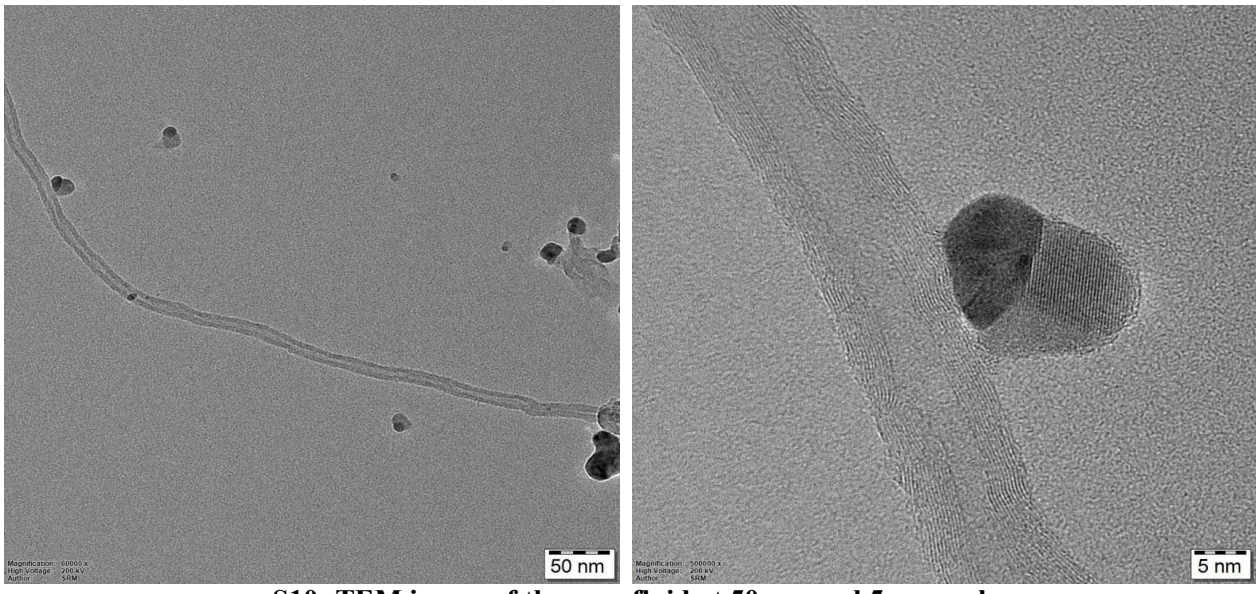

S10: TEM image of the nanofluid at 50 nm and 5 nm scale

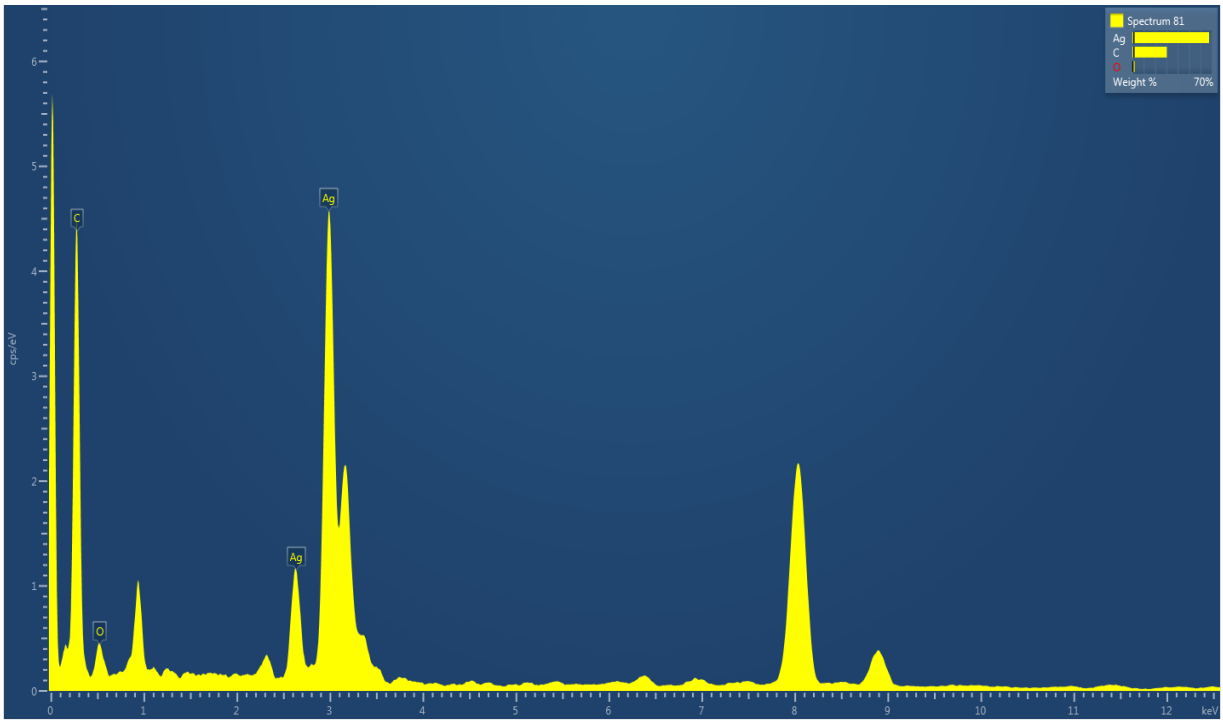

S11: EDX spectrum for the TEM

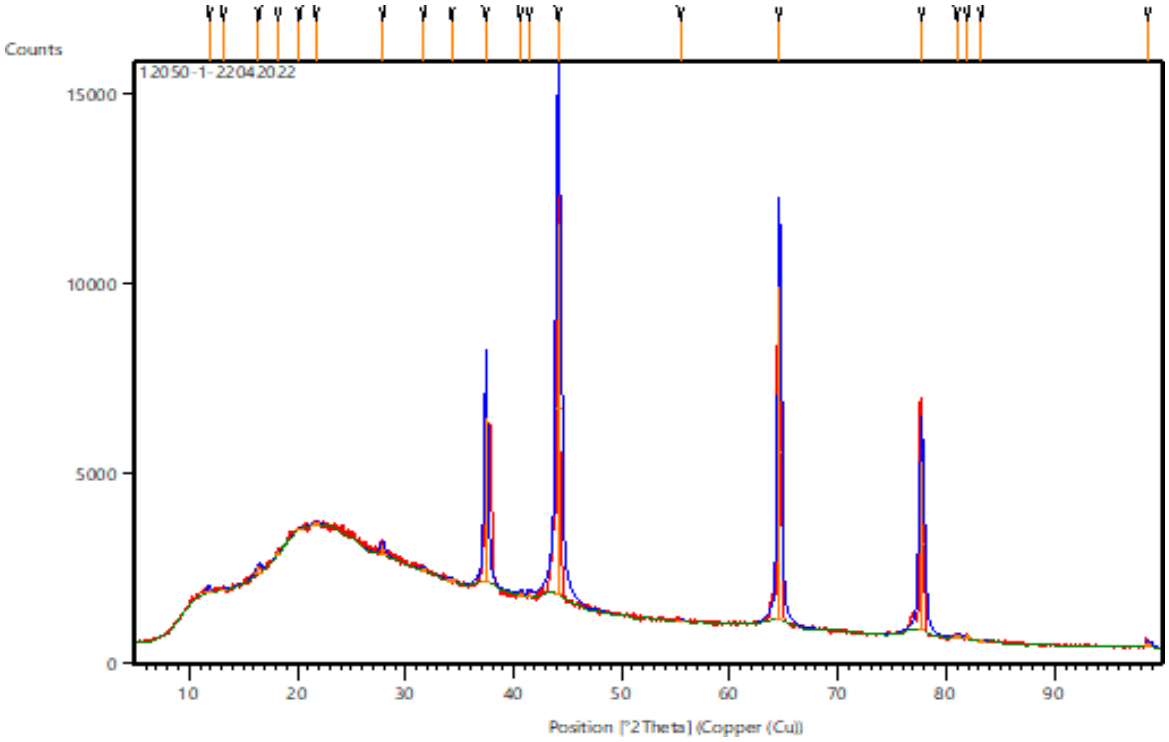

Pos.[°2Th.]	Height [cts]	FWHM Left[°2Th.]	d-spacing [Å]	Rel. Int. [%]
11.8427	130.99	0.3464	7.47297	1.34
13.1214	4.73	0.5196	6.74746	0.05
16.4183	199.59	0.5196	5.39920	2.05
18.2359	49.92	0.3464	4.86496	0.51
20.1681	21.49	0.6927	4.40303	0.22
21.6824	61.35	0.6927	4.09881	0.63
27.8831	247.19	0.5196	3.19981	2.54
31.6642	93.07	0.3464	2.82581	0.96
34.2643	53.01	1.0391	2.61710	0.54
38.0498	4327.42	0.3464	2.40149	44.41
40.6017	84.34	0.3464	2.22204	0.87
41.4681	117.02	0.3464	2.17760	1.20
44.1212	9744.41	0.5196	2.05262	100.00
55.4596	67.74	0.3464	1.65685	0.70
64.5510	8806.42	0.3464	1.44373	90.37
77.6959	4453.73	0.4330	1.22906	45.71
81.0263	82.46	0.4330	1.18675	0.85
81.9294	77.27	0.3464	1.17594	0.79
83.2663	35.87	0.5196	1.16042	0.37
98.6631	141.87	0.5196	1.01641	1.46

S12: XRD results for Ternary Nanofluid and their Peak list.

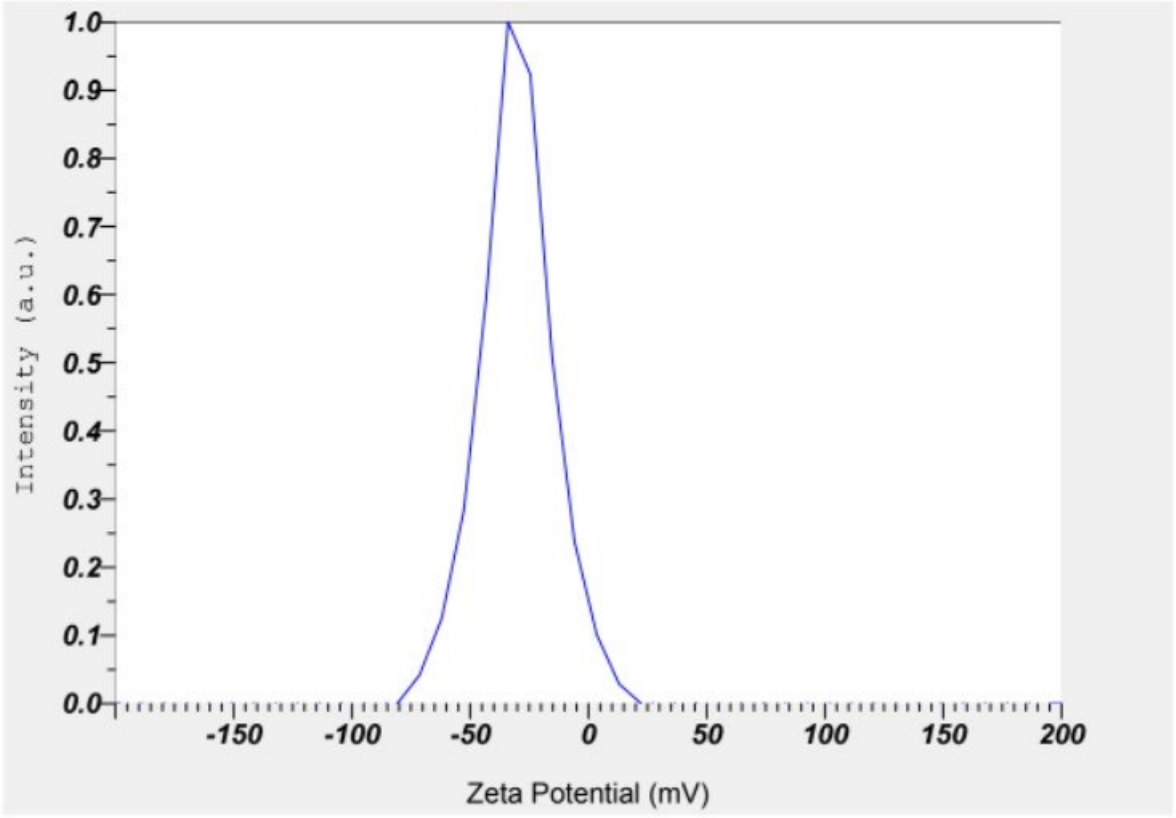

S13: Zeta Potential of nanofluid after 15 days